EChOes from gravitational waves

Alfredo Urbano, CERN

DESY, 4 April 2016

with G. F. Giudice and M. McCullough

PART I

INTRODUCTION

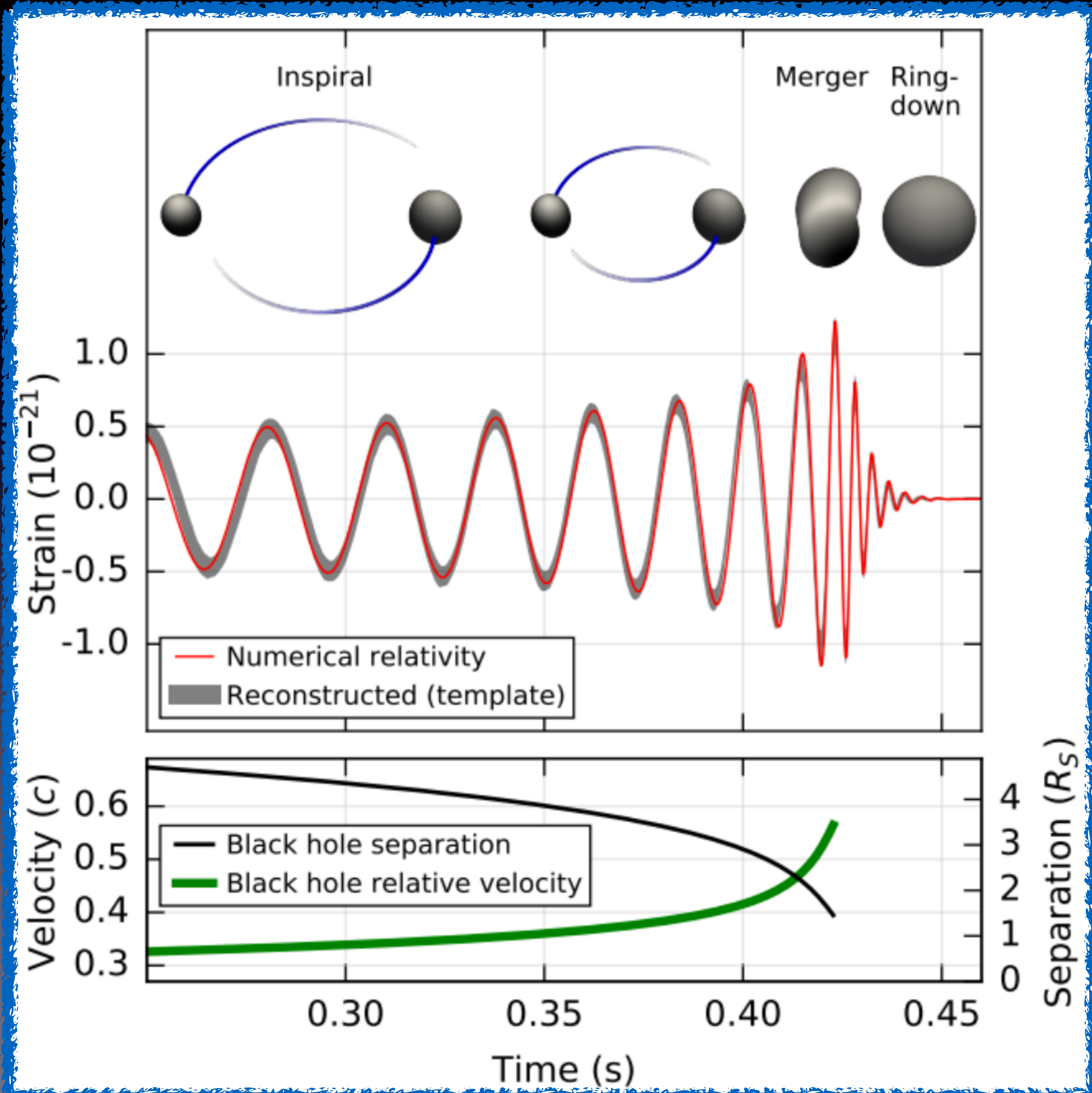
Inspiral
Merger
Ring-
down
1.0
0.5
0.0
-0.5
-1.0
Strain (10^{-21})
Numerical relativity
Reconstructed (template)
0.6
0.5
0.4
0.3
Velocity (c)
Black hole separation
Black hole relative velocity
4
3
2
1
0
Separation (R_S)
0.30
0.35
0.40
0.45
Time (s)

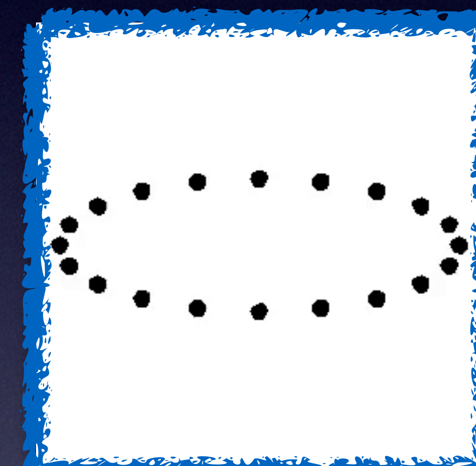

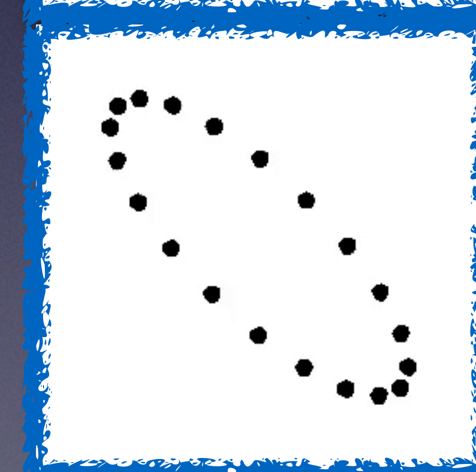

$$M = M_1 + M_2\ , \qquad \mu = \frac{M_1 M_2}{M} \qquad \Longrightarrow \qquad \Omega^2 = \left(\frac{2\pi}{P}\right)^2 = \frac{G_N M}{a^3}$$

$$E = -\frac{G_N \mu M}{2a}$$

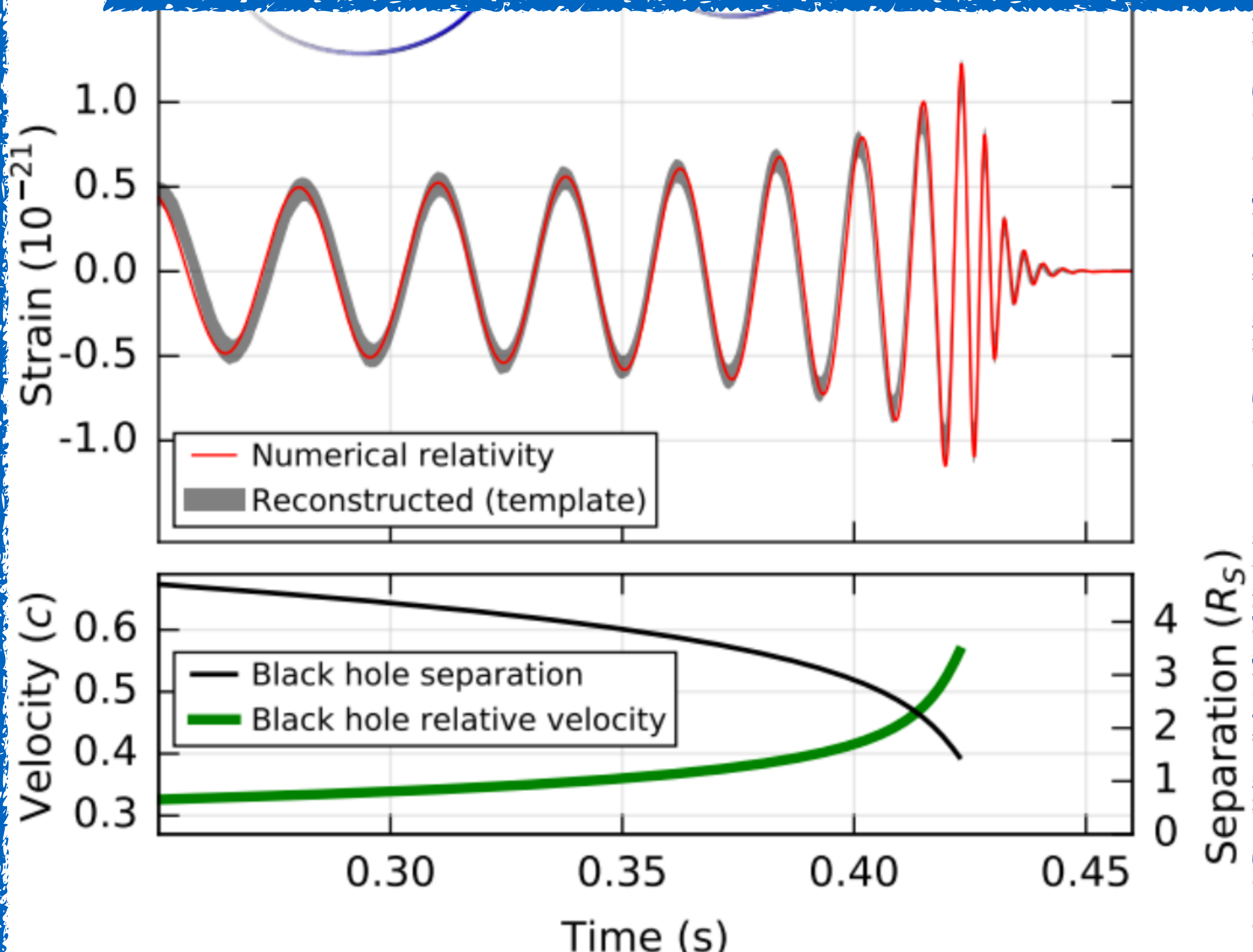

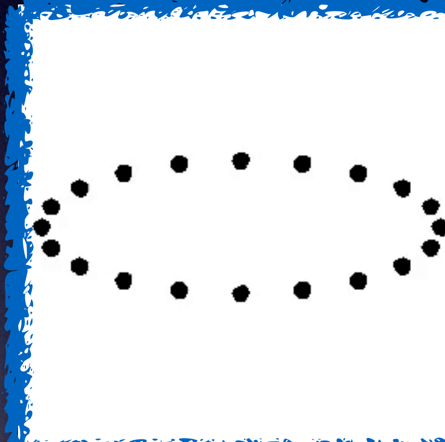

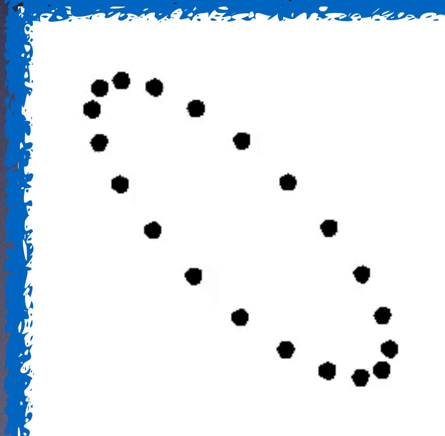

$$M = M_1 + M_2\ , \qquad \mu = \frac{M_1 M_2}{M} \qquad \Longrightarrow \qquad \Omega^2 = \left(\frac{2\pi}{P}\right)^2 = \frac{G_N M}{a^3}$$

$$E = -\frac{G_N \mu M}{2a}$$

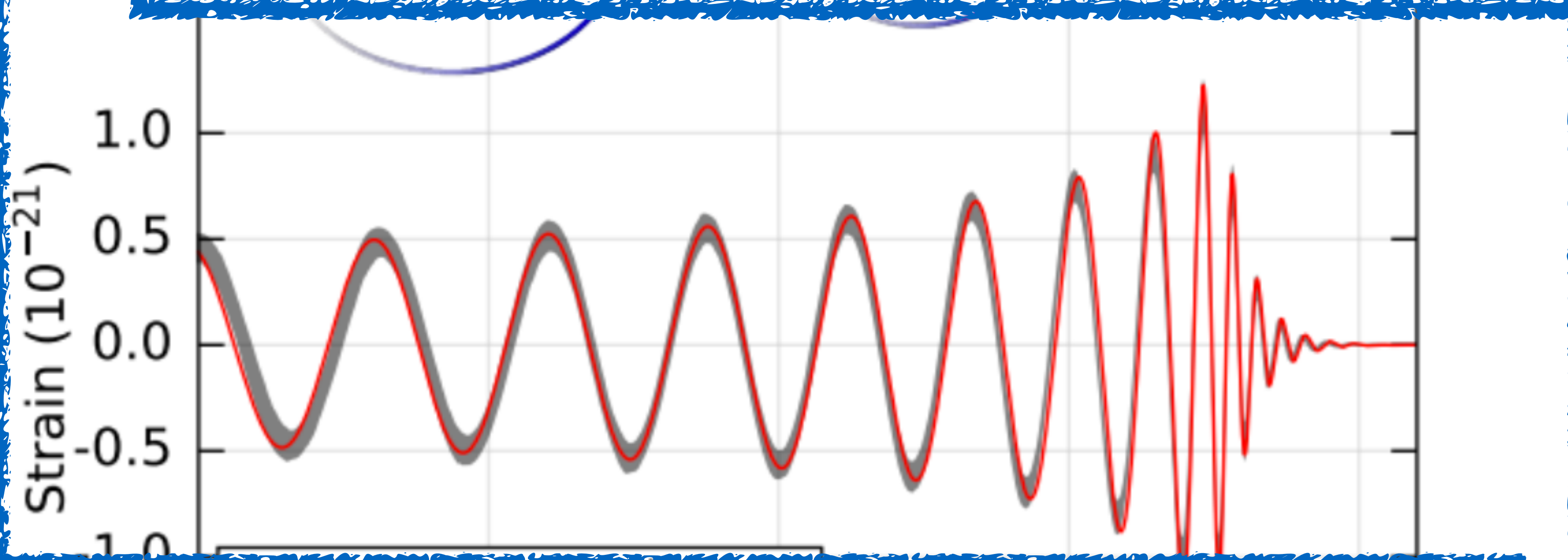

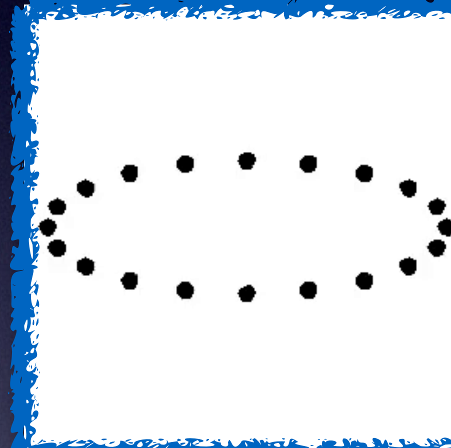

$$h_+ \;=\; \frac{2G_N^{5/3}}{rc^4}(1+\cos^2 i)(\pi f M)^{2/3}\mu\cos(2\pi f t)$$

$$h_\times \;=\; \frac{G_N^{5/3}}{rc^4} 4\cos i(\pi f M)^{2/3}\mu\sin(2\pi f t)$$

$$f = \frac{\Omega}{\pi} = \sqrt{\frac{M}{\pi^2 a^3}}$$

$$\mu M^{2/3} = M_C^{5/3} \qquad \Longrightarrow \qquad M_C \equiv \mu^{3/5} M^{2/5}$$

aLIGO noise power spectral density

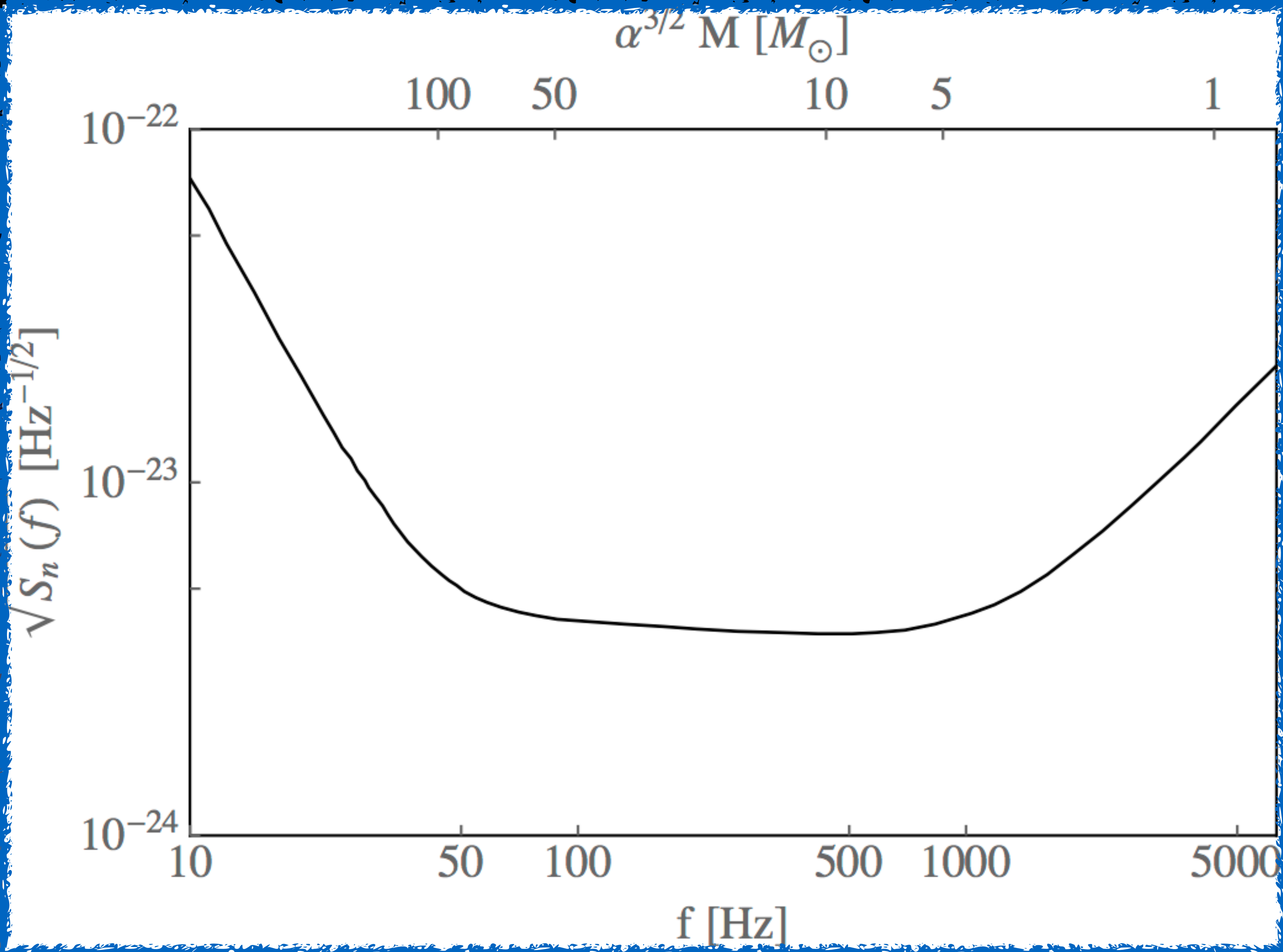

P.Ajith, arXiv:1107.1267

aLIGO noise power spectral density

$$f_{\rm ISCO} = \frac{1}{6^{3/2}\pi M} \quad \Longrightarrow \quad 4\,M_\odot \lesssim M \lesssim 90\,M_\odot$$

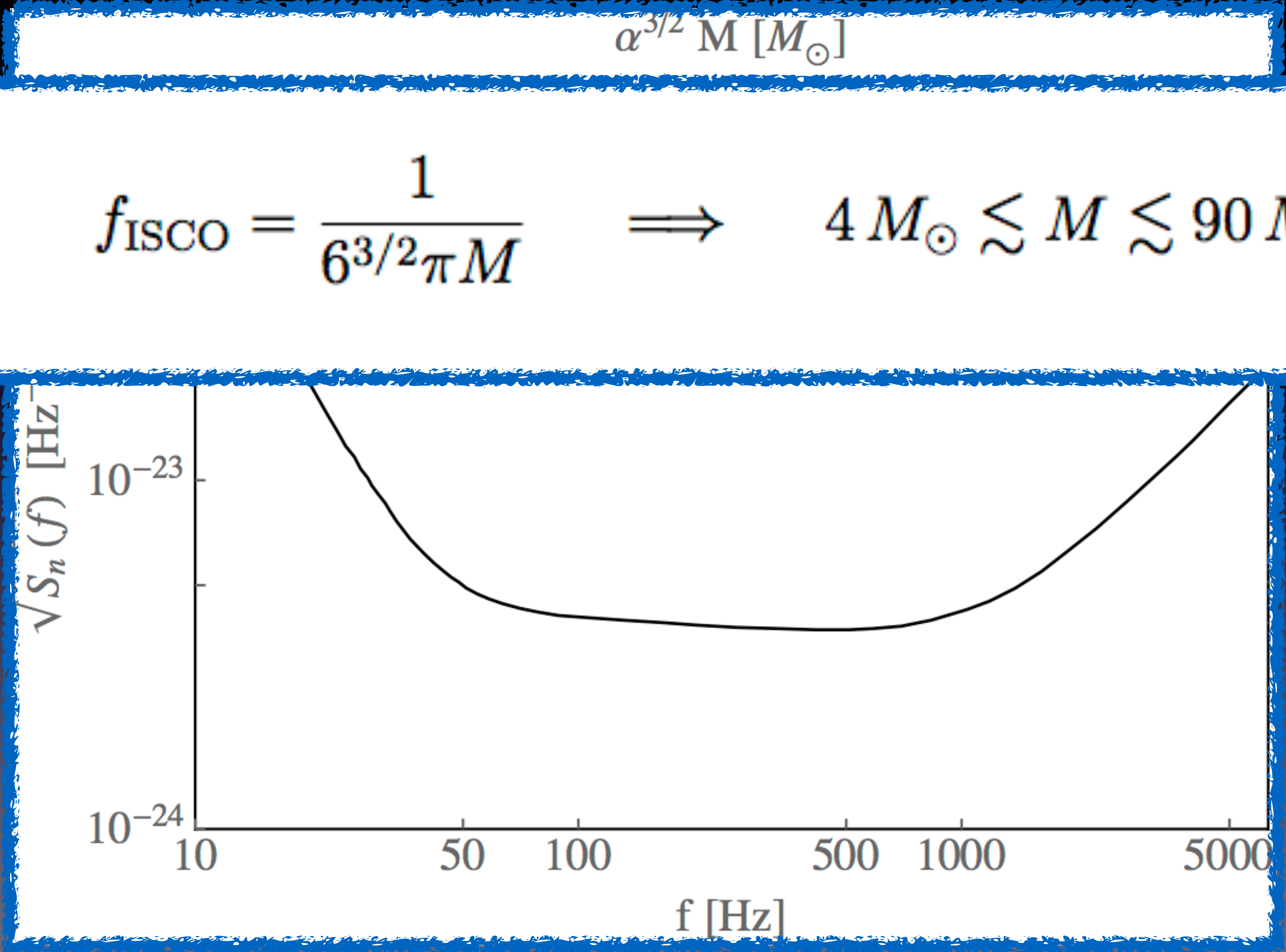

P.Ajith, arXiv:1107.1267

TABLE I. Summary of the parameters that characterise GW150914. For model parameters we report the median value as well as the range of the symmetric 90% credible interval [86]; where useful, we also quote 90% credible bounds. For the logarithm of the Bayes factor for a signal compared to Gaussian noise we report the mean and its 90% standard error from 4 parallel runs with a nested sampling algorithm [45]. The source redshift and source-frame masses assume standard cosmology [87]. The spin-aligned EOBNR and precessing IMRPhenom waveform models are described in the text. Results for the effective precession spin parameter χ_p used in the IMRPhenom model are not shown as we effectively recover the prior; we constrain $\chi_\mathrm{p} < 0.81$ at 90% probability, see left panel of Figure 5. The Overall results are computed by averaging the posteriors for the two models. For the Overall results we quote both the 90% credible interval or bound and an estimate for the 90% range of systematic error on this determined from the variance between waveform models.

	EOBNR	IMRPhenom	Overall
Detector-frame total mass $M/\mathrm{M}_\odot$	$70.3^{+5.3}_{-4.8}$	$70.7^{+3.8}_{-4.0}$	$70.5^{+4.6\pm0.9}_{-4.5\pm1.0}$
Detector-frame chirp mass $\mathcal{M}/\mathrm{M}_\odot$	$30.2^{+2.5}_{-1.9}$	$30.5^{+1.7}_{-1.8}$	$30.3^{+2.1\pm0.4}_{-1.9\pm0.4}$
Detector-frame primary mass $m_1/\mathrm{M}_\odot$	$39.4^{+5.5}_{-4.9}$	$38.3^{+5.5}_{-3.5}$	$38.8^{+5.6\pm0.9}_{-4.1\pm0.3}$
Detector-frame secondary mass $m_2/\mathrm{M}_\odot$	$30.9^{+4.8}_{-4.4}$	$32.2^{+3.6}_{-5.0}$	$31.6^{+4.2\pm0.1}_{-4.9\pm0.6}$
Detector-frame final mass $M_\mathrm{f}/\mathrm{M}_\odot$	$67.1^{+4.6}_{-4.4}$	$67.4^{+3.4}_{-3.6}$	$67.3^{+4.1\pm0.8}_{-4.0\pm0.9}$
Source-frame total mass $M^\mathrm{source}/\mathrm{M}_\odot$	$65.0^{+5.0}_{-4.4}$	$64.6^{+4.1}_{-3.5}$	$64.8^{+4.6\pm1.0}_{-3.9\pm0.5}$
Source-frame chirp mass $\mathcal{M}^\mathrm{source}/\mathrm{M}_\odot$	$27.9^{+2.3}_{-1.8}$	$27.9^{+1.8}_{-1.6}$	$27.9^{+2.1\pm0.4}_{-1.7\pm0.2}$
Source-frame primary mass $m_1^\mathrm{source}/\mathrm{M}_\odot$	$36.3^{+5.3}_{-4.5}$	$35.1^{+5.2}_{-3.3}$	$35.7^{+5.4\pm1.1}_{-3.8\pm0.0}$
Source-frame secondary mass $m_2^\mathrm{source}/\mathrm{M}_\odot$	$28.6^{+4.4}_{-4.2}$	$29.5^{+3.3}_{-4.5}$	$29.1^{+3.8\pm0.2}_{-4.4\pm0.5}$
Source-fame final mass $M_\mathrm{f}^\mathrm{source}/\mathrm{M}_\odot$	$62.0^{+4.4}_{-4.0}$	$61.6^{+3.7}_{-3.1}$	$61.8^{+4.2\pm0.9}_{-3.5\pm0.4}$
Mass ratio q	$0.79^{+0.18}_{-0.19}$	$0.84^{+0.14}_{-0.21}$	$0.82^{+0.16\pm0.01}_{-0.21\pm0.03}$
Effective inspiral spin parameter χ_eff	$0.09^{+0.19}$	$0.03^{+0.14}$	$0.06^{+0.17\pm0.01}$
Dimensionless primary spin magnitude a_1	$0.32^{+0.45}_{-0.28}$	$0.31^{+0.51}_{-0.27}$	$0.31^{+0.48\pm0.04}_{-0.28\pm0.01}$
Dimensionless secondary spin magnitude a_2	$0.57^{+0.40}_{-0.51}$	$0.39^{+0.50}_{-0.34}$	$0.46^{+0.48\pm0.07}_{-0.42\pm0.01}$
Final spin a_f	$0.67^{+0.06}_{-0.08}$	$0.67^{+0.05}_{-0.05}$	$0.67^{+0.05\pm0.00}_{-0.07\pm0.03}$
Luminosity distance $D_\mathrm{L}/\mathrm{Mpc}$	390^{+170}_{-180}	440^{+140}_{-180}	$410^{+160\pm20}_{-180\pm40}$
Source redshift z	$0.083^{+0.033}_{-0.036}$	$0.093^{+0.028}_{-0.036}$	$0.088^{+0.031\pm0.004}_{-0.038\pm0.009}$
Upper bound on primary spin magnitude a_1	0.65	0.71	0.69 ± 0.05
Upper bound on secondary spin magnitude a_2	0.93	0.81	0.88 ± 0.10
Lower bound on mass ratio q	0.64	0.67	0.65 ± 0.03
Log Bayes factor $\ln \mathcal{B}_{\mathrm{s/n}}$	288.7 ± 0.2	290.1 ± 0.2	—

https://www.black-holes.org/waveforms/

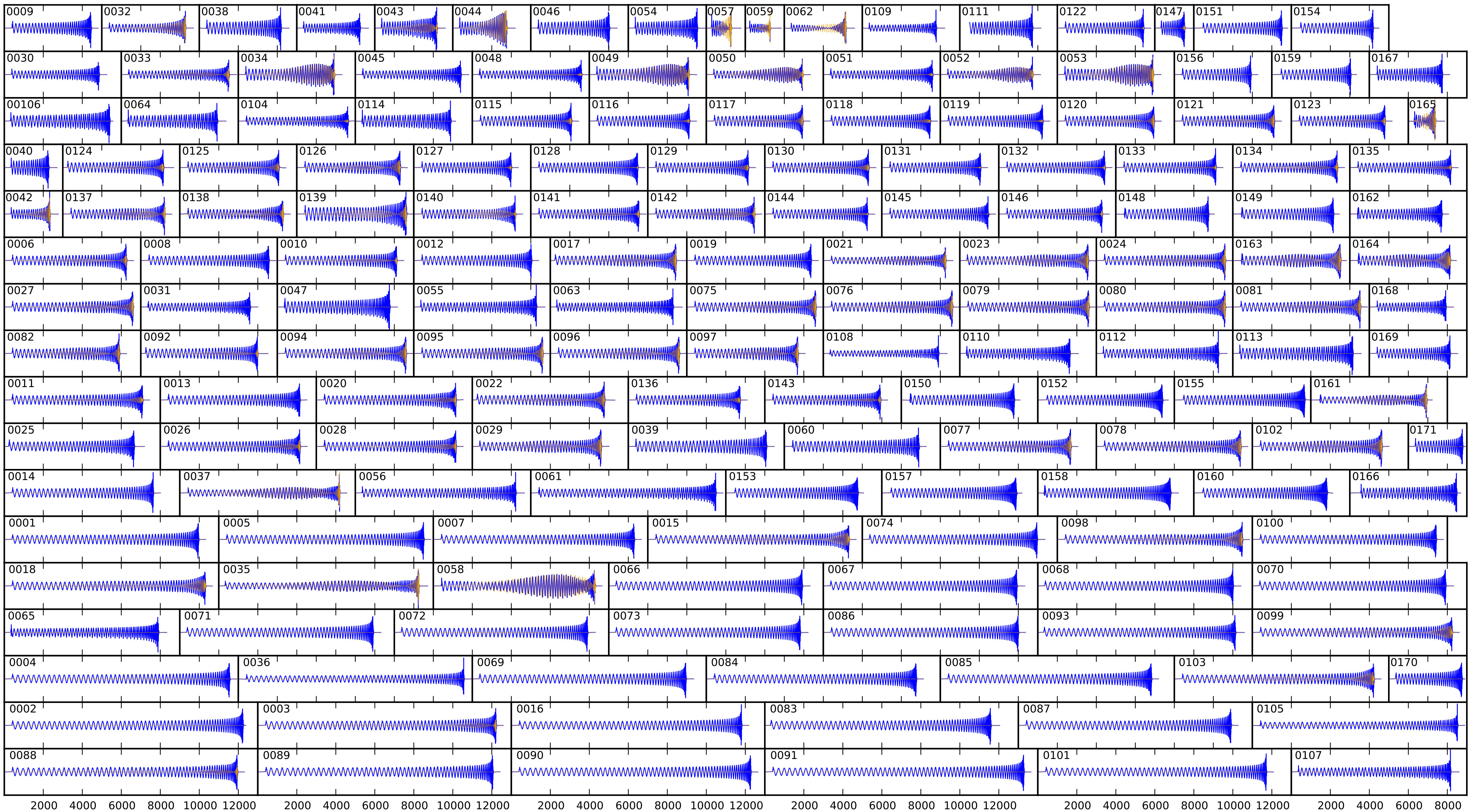

arXiv:1304.6077

PART II

TEST OF GR

Test of GR

Ellis, Mavromatos, Nanopoulos, arXiv:1602.04764
Lorentz violation in graviton propagation

Blas, Ivanov, Sawicki, Sibiryakov, arXiv:1602.04188
Upper bound (1.7) on the speed of propagation of gravitational waves

LIGO Scientific and Virgo collaborations, arXiv:1602.03841
Bound on graviton mass

cfr. Yunes, Yagi, Pretorius, arXiv:1603.08955
for a comprehensive analysis of possible implications

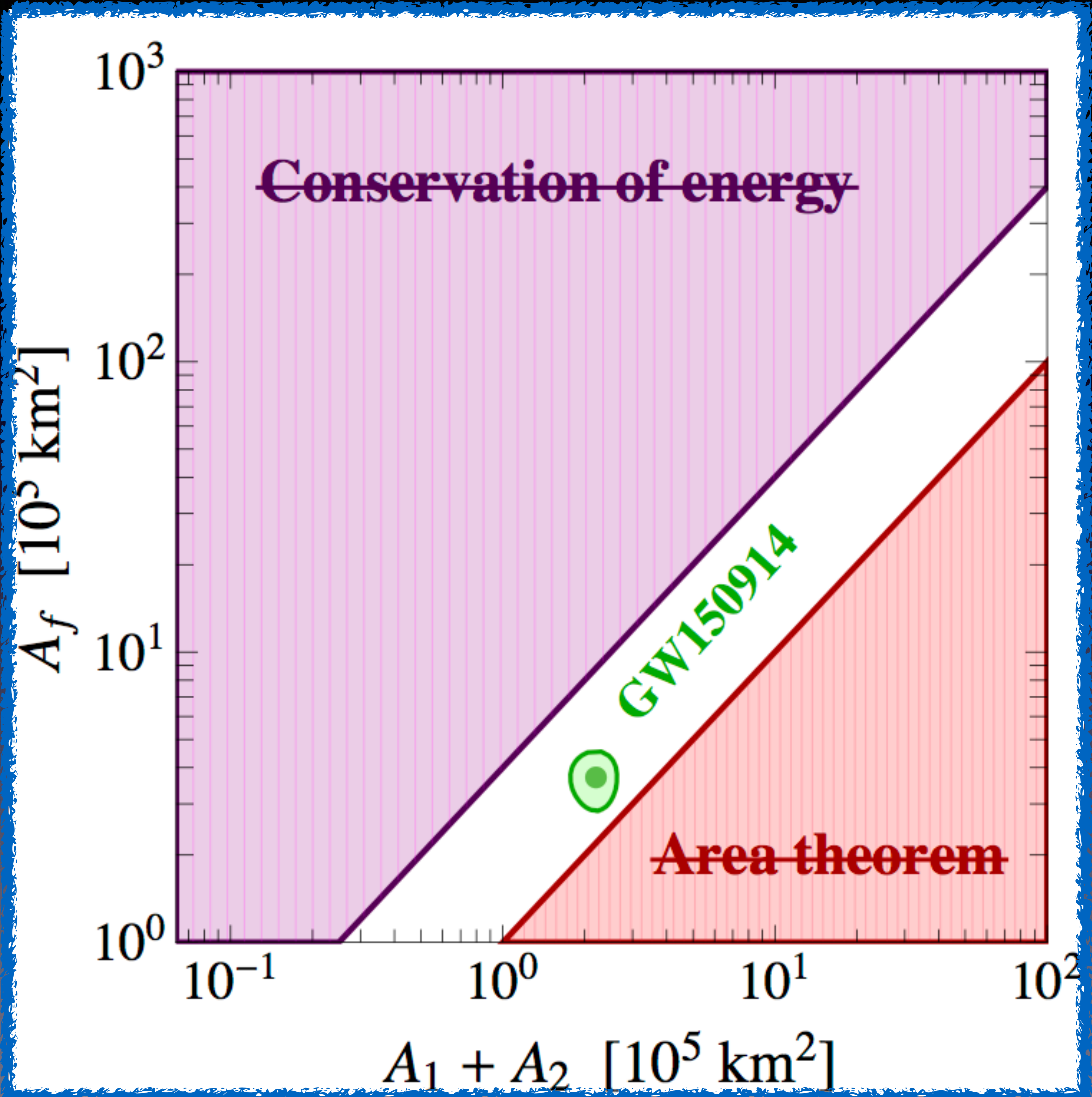

Conservation of energy
GW150914
Area theorem
A_f [10^5 km^2]
$A_1 + A_2$ [10^5 km^2]
10^0
10^1
10^2
10^3
10^{-1}

PART III

EXOTIC COMPACT OBJETCS

(waveform)

Neutron Star merger

"Neutron stars are compact stars (radius ~10 km). They can result from the gravitational collapse of a massive star. Neutron stars are composed almost entirely of neutrons. They are supported against further collapse by quantum degeneracy pressure due to the phenomenon described by the Pauli exclusion principle."

Wikipedia
The Free Encyclopedia

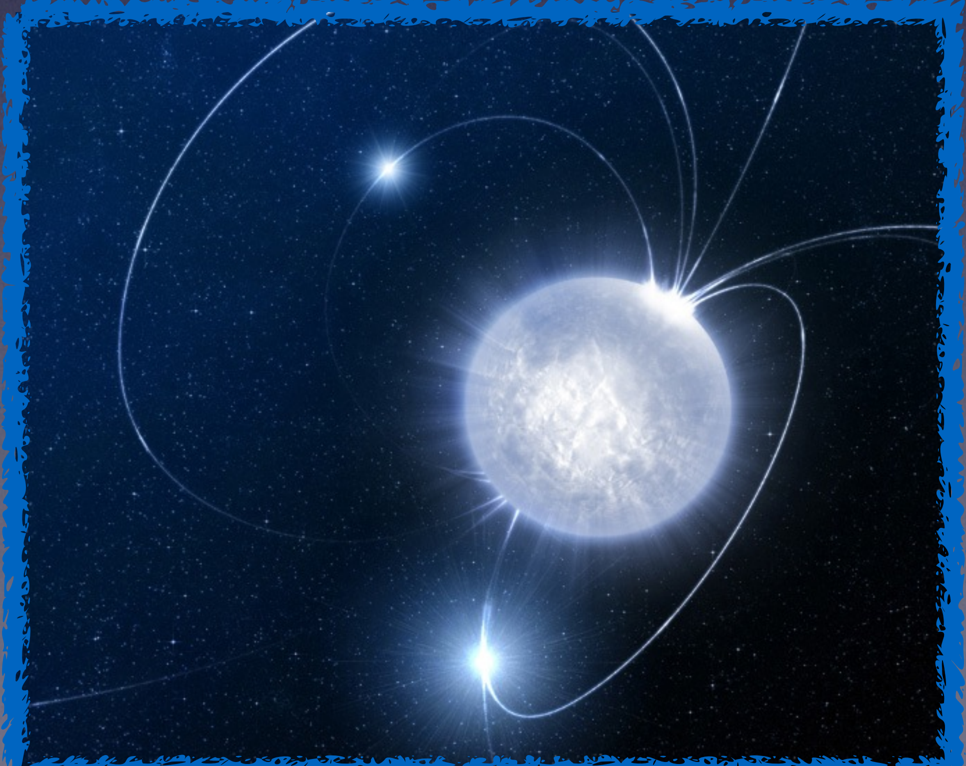

On the existence of a "mass gap"

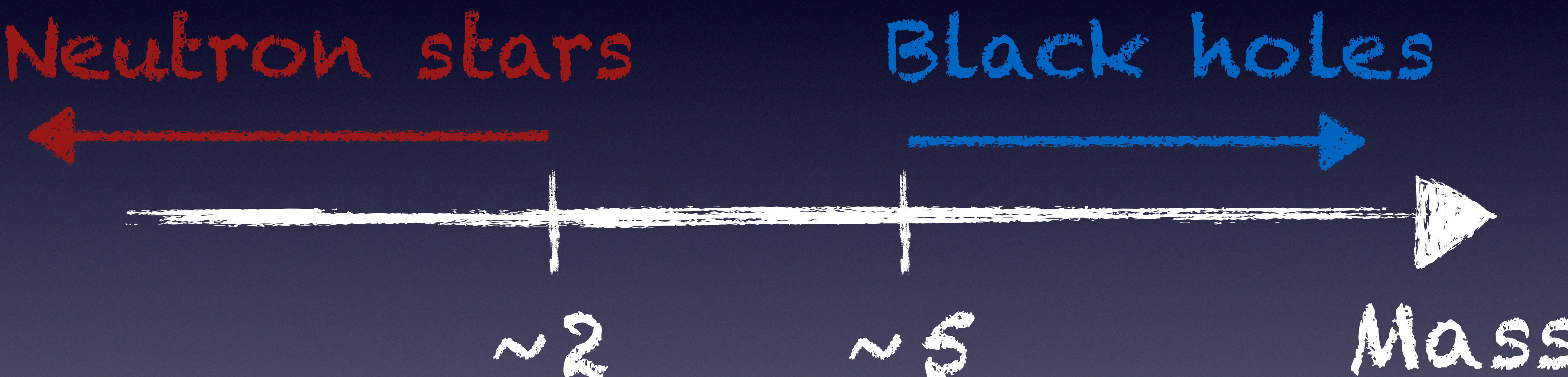

Typical compactness
$C = M/R = [0.1-0.2]$
($C = 0.5$ for a Schw. BH)

Neutron star binaries waveform

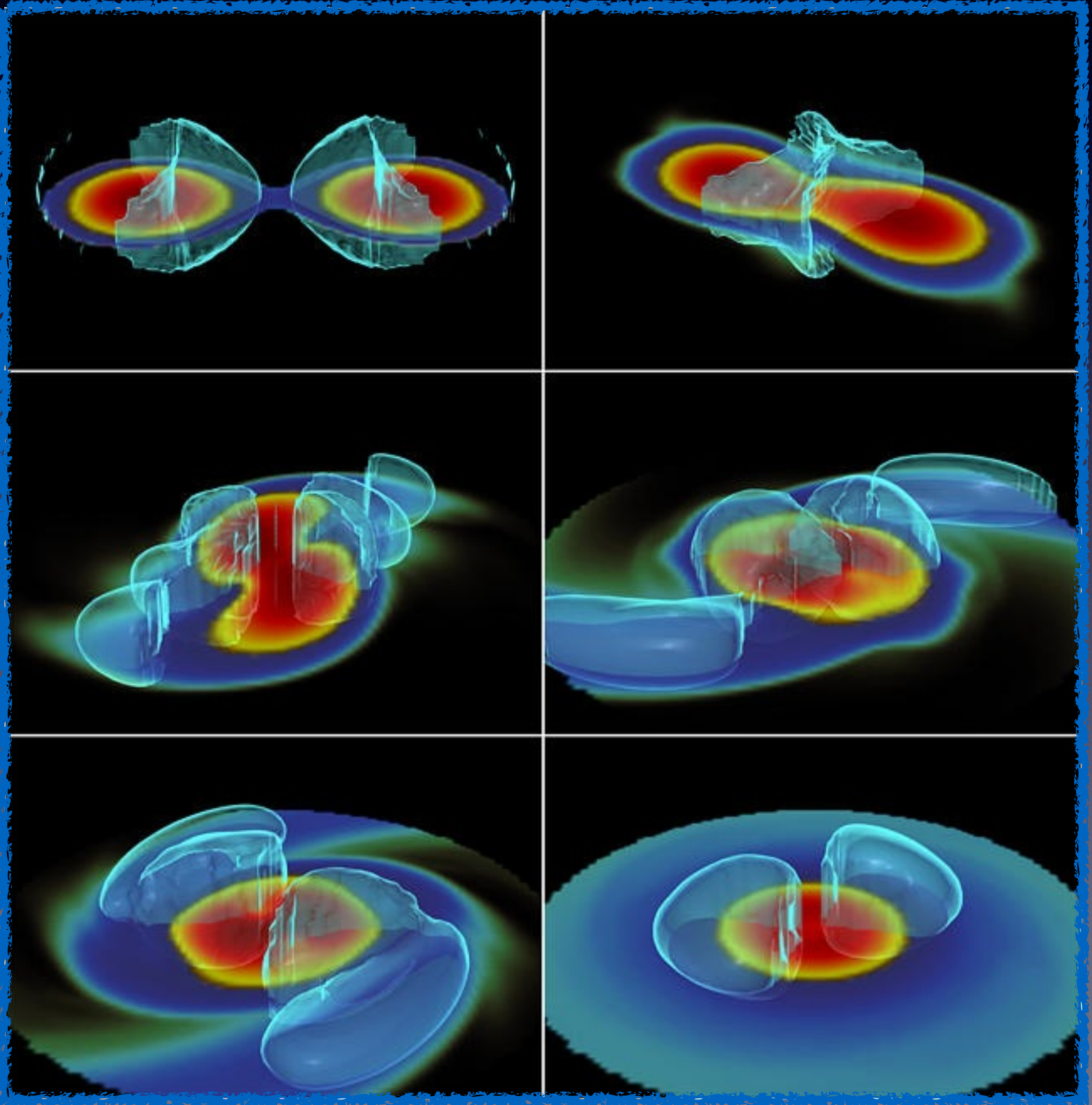

Polytrope with Gamma = [2-3]

Neutron star binaries waveform

Ruffert, Janka
astro-ph/0106229

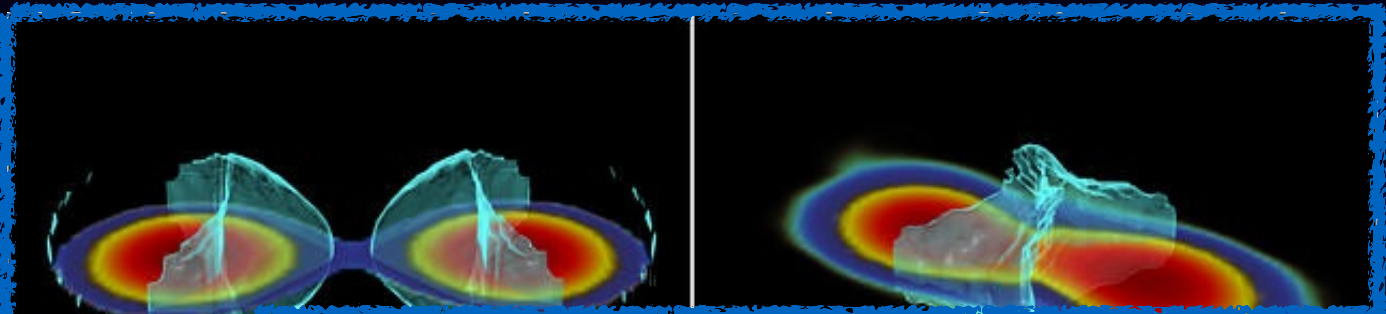

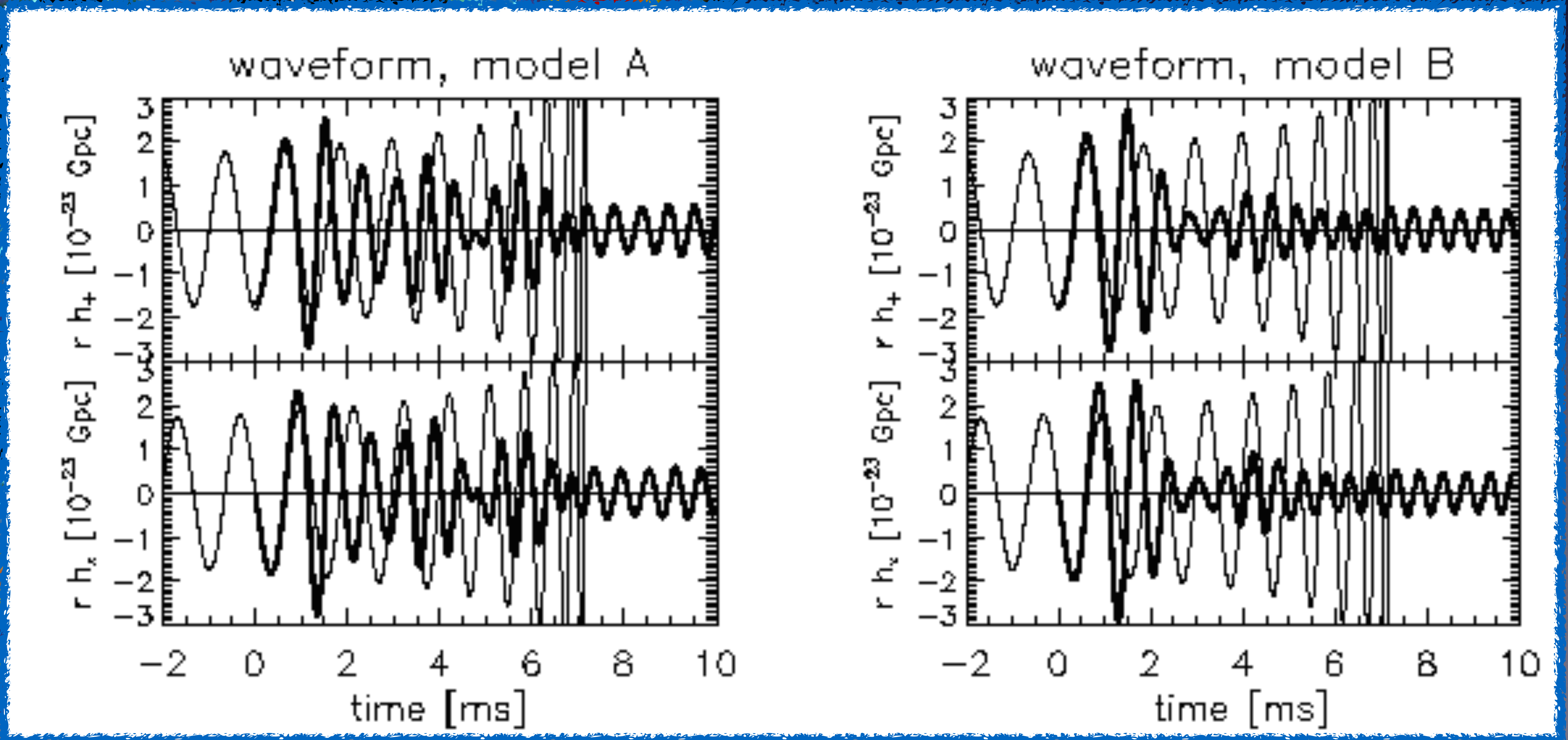

Exotic Compact Objects

Boson stars

Axions, axion-like particles, moduli, flat directions...

Fermion stars

Asymmetric self-interacting dark matter, unconventional states of ordinary matter, "mirror world" (twin Higgs)..

Dark energy stars

MACHOs

MAssive Compact Halo Objets

Observational constraint from micro lensing events

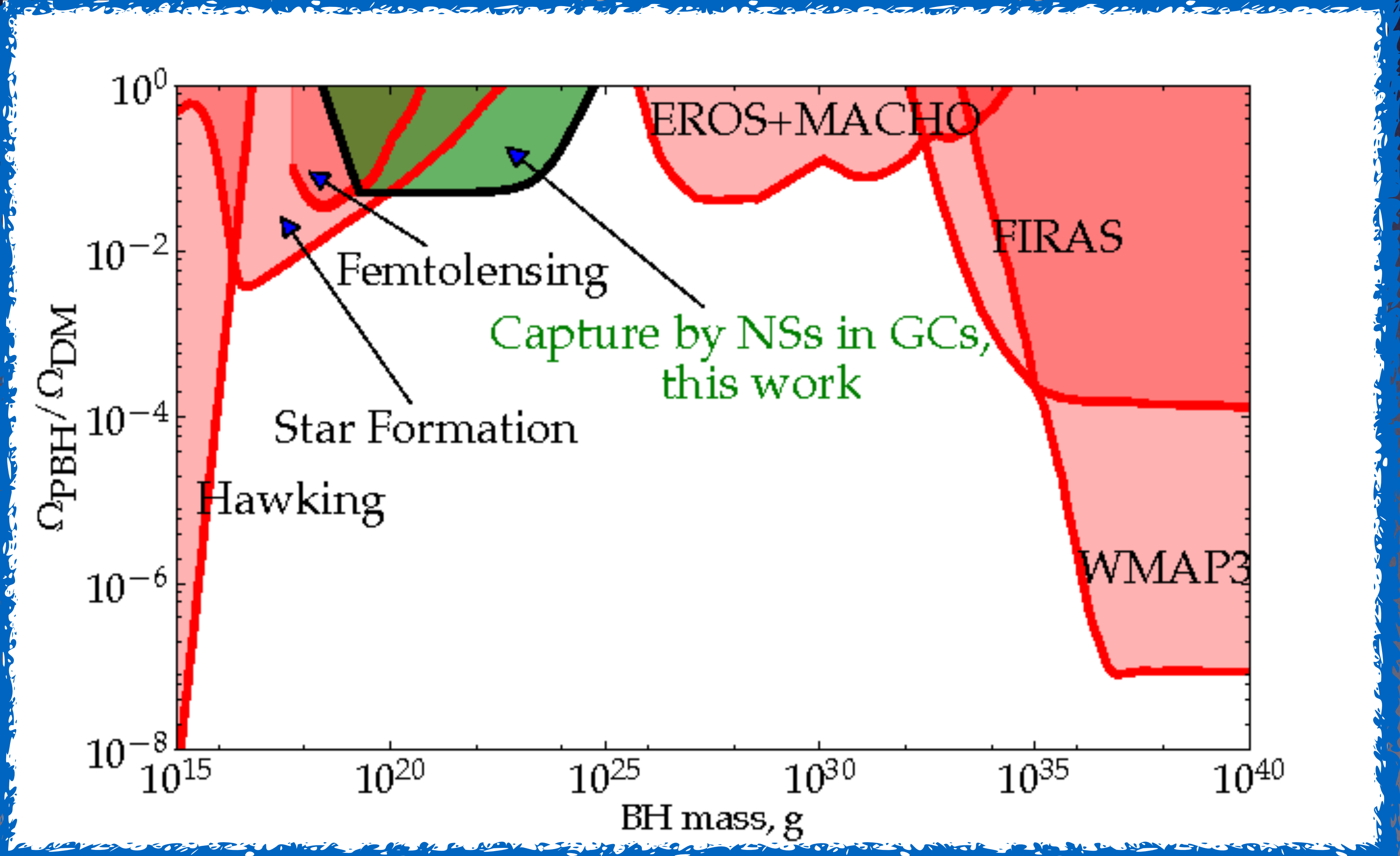

Boson star

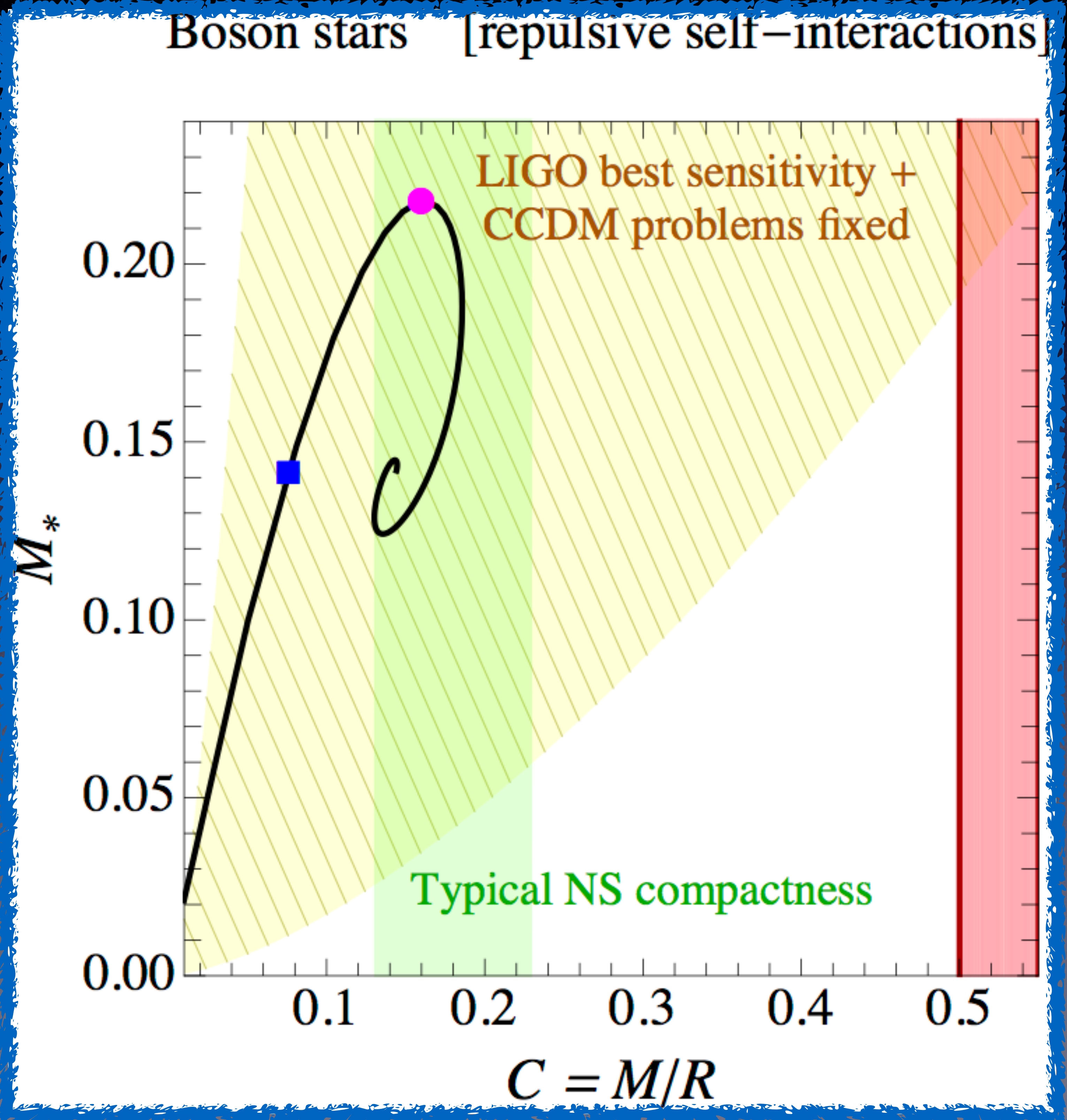
Boson stars [repulsive self−interactions]
LIGO best sensitivity +
CCDM problems fixed
Typical NS compactness
0.00
0.05
0.10
0.15
0.20
M_*
0.1
0.2
0.3
0.4
0.5
$C = M/R$

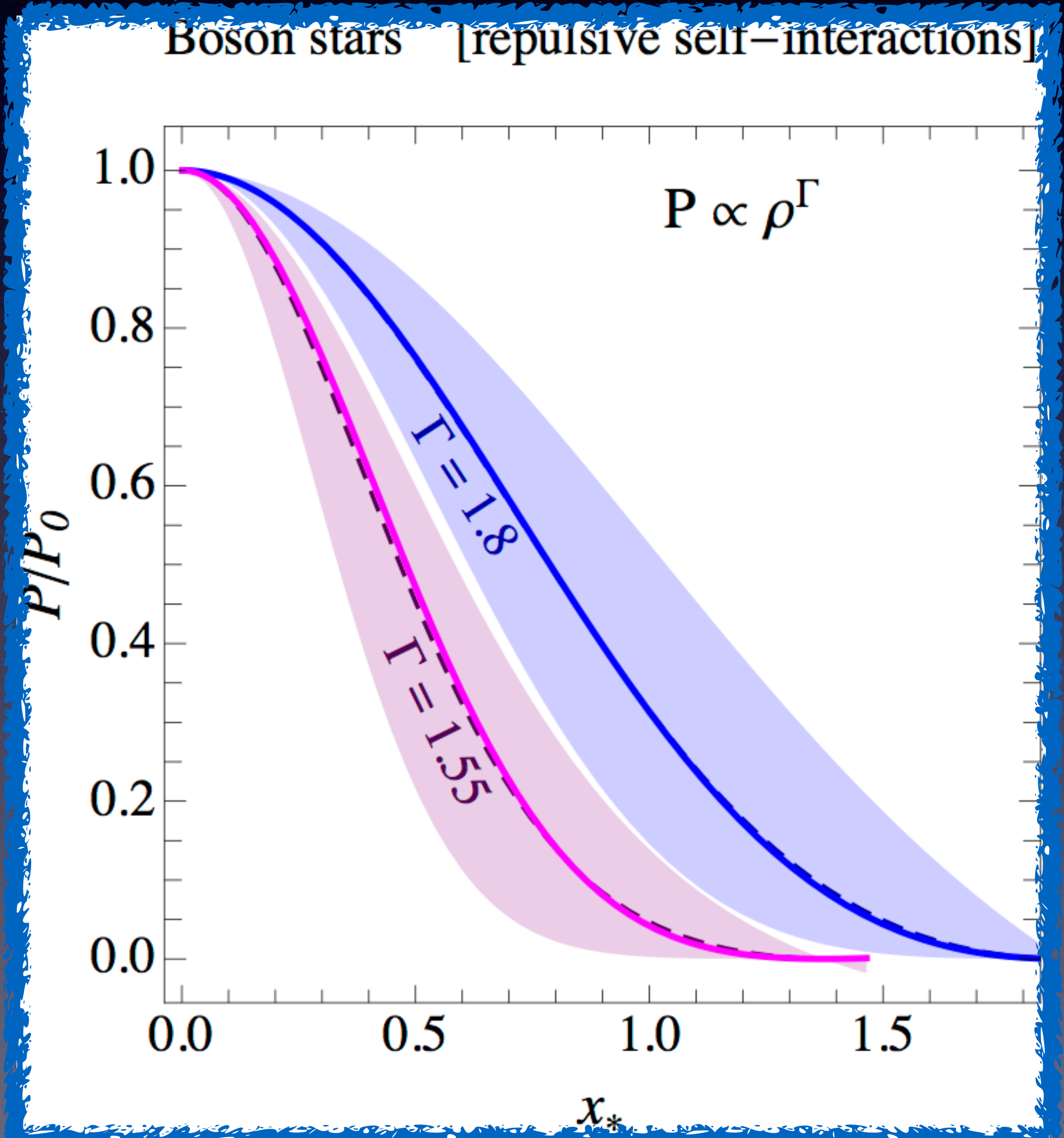
Boson stars [repulsive self−interactions]
$P \propto \rho^\Gamma$
$\Gamma = 1.8$
$\Gamma = 1.55$
P/P_0
0.0
0.2
0.4
0.6
0.8
1.0
0.0
0.5
1.0
1.5
x_*

Boson star binaries waveform

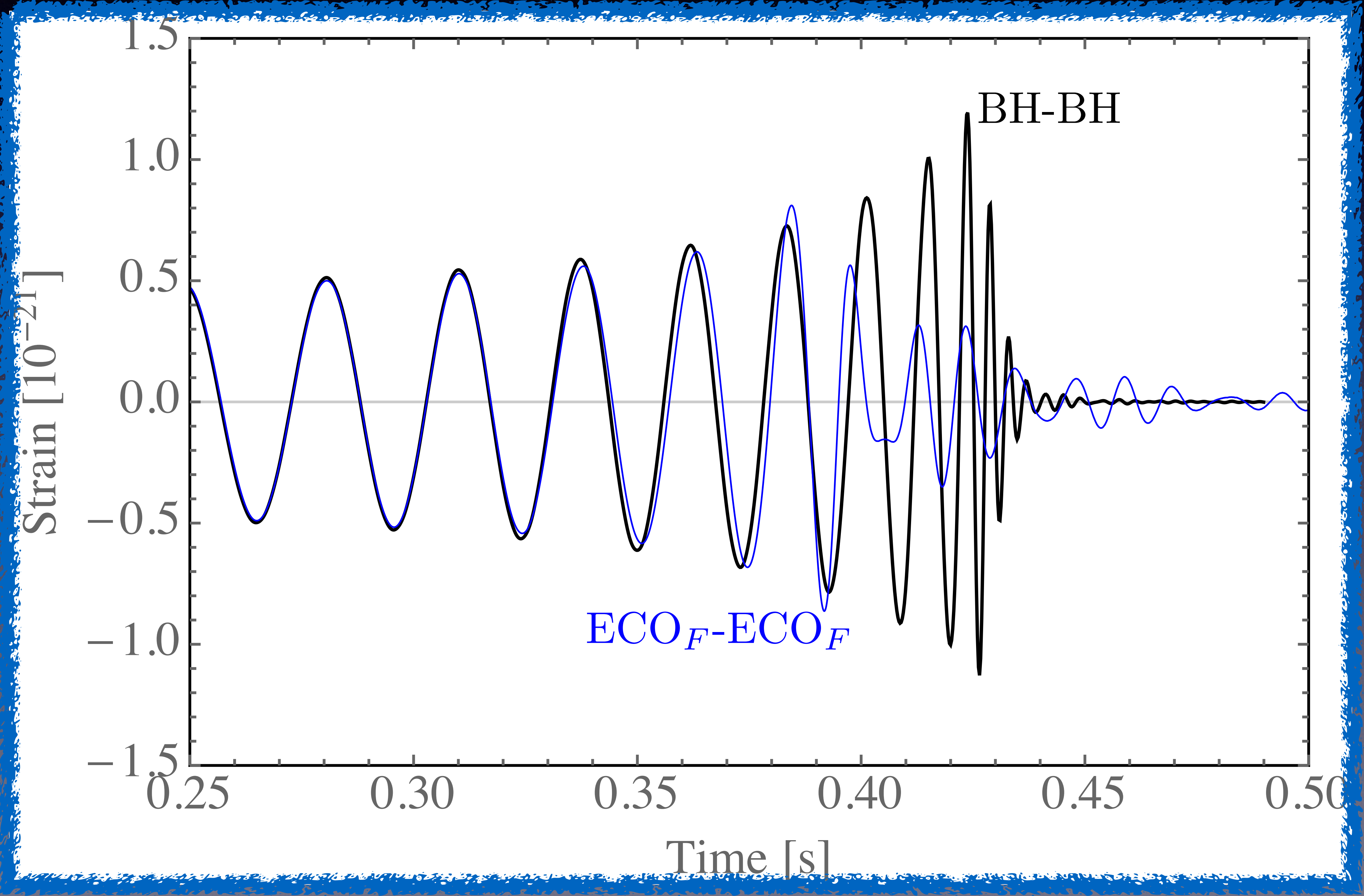

Boson star binaries waveform

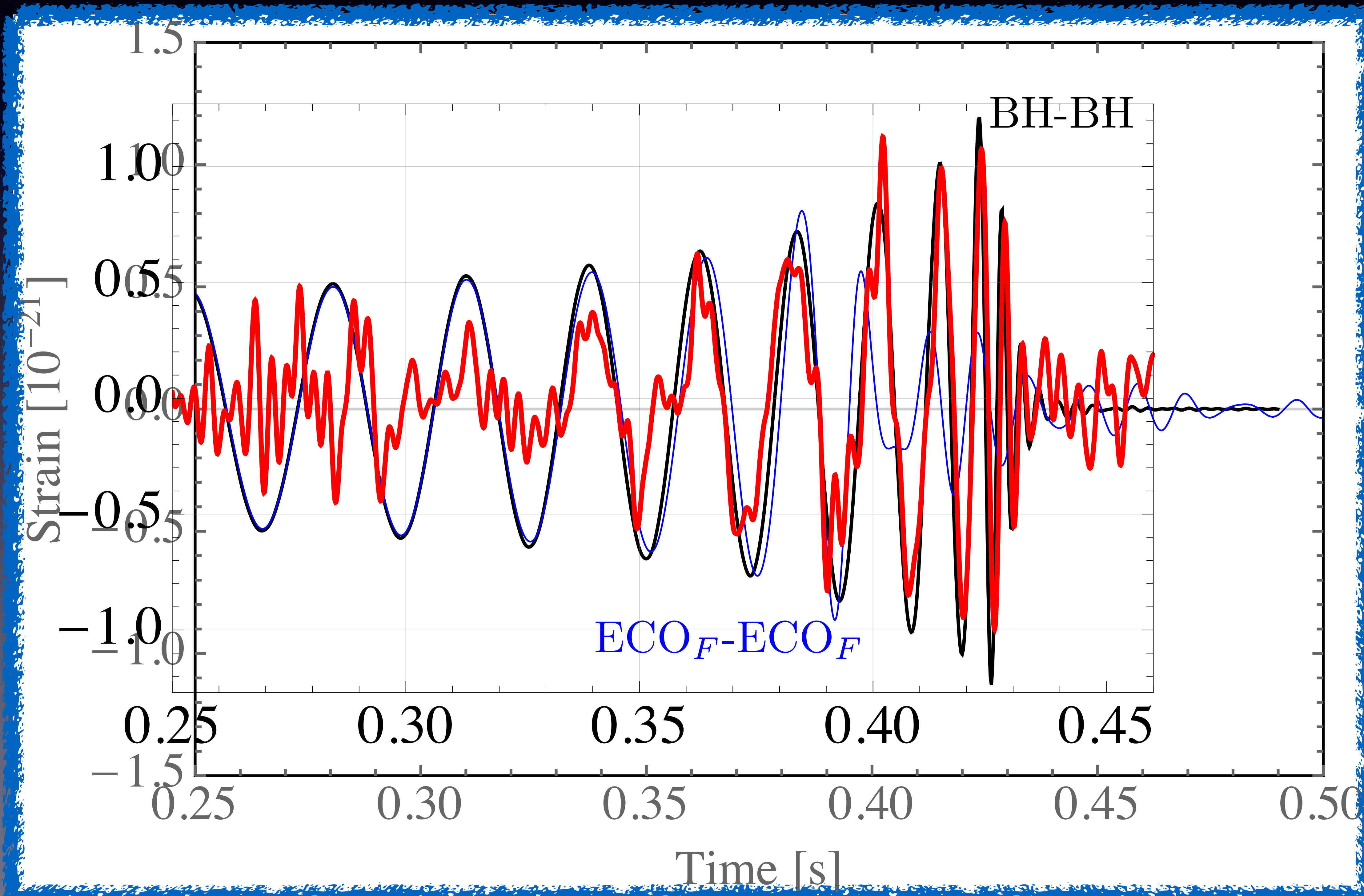

Ringdown phase

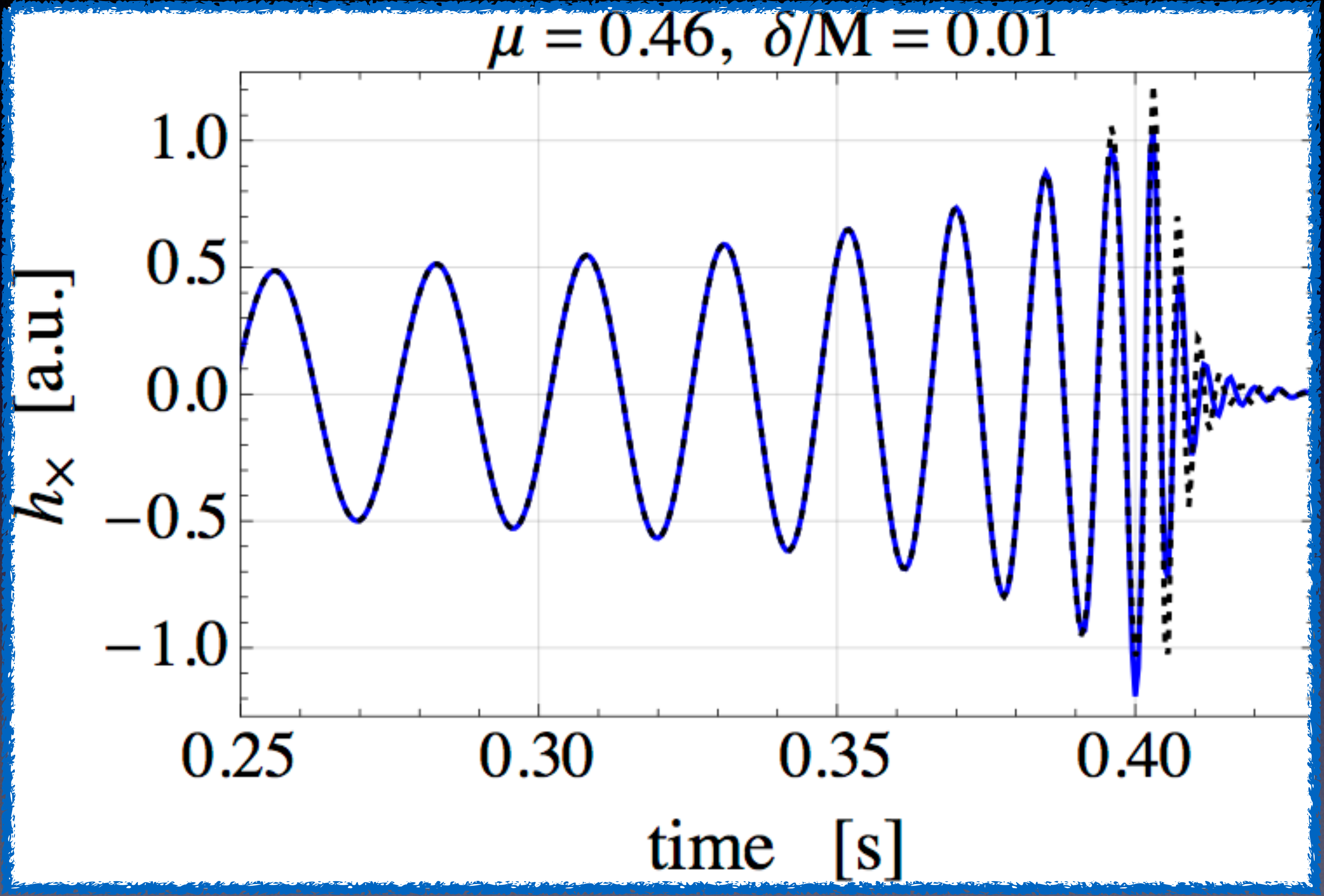

Ringdown phase

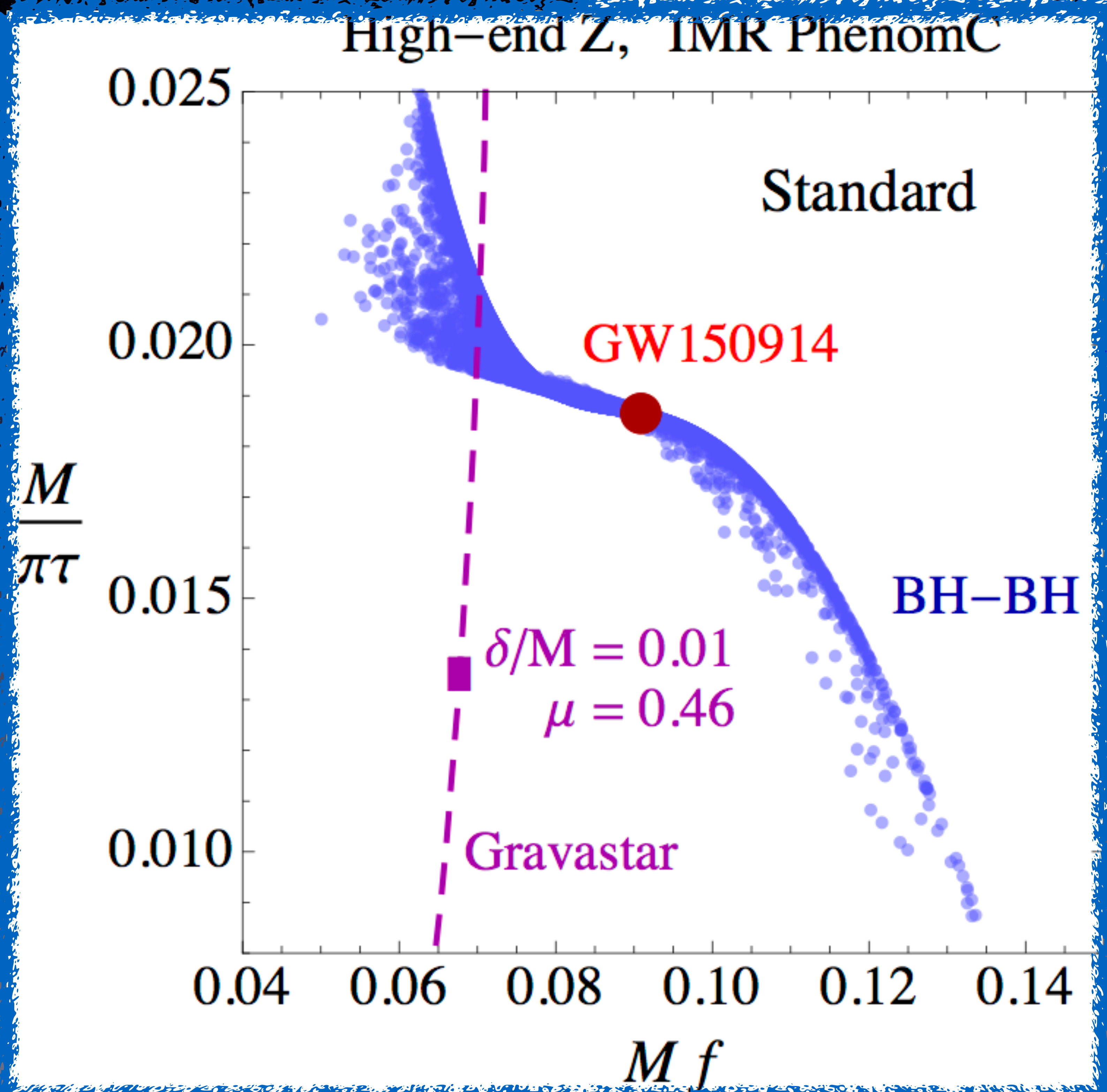

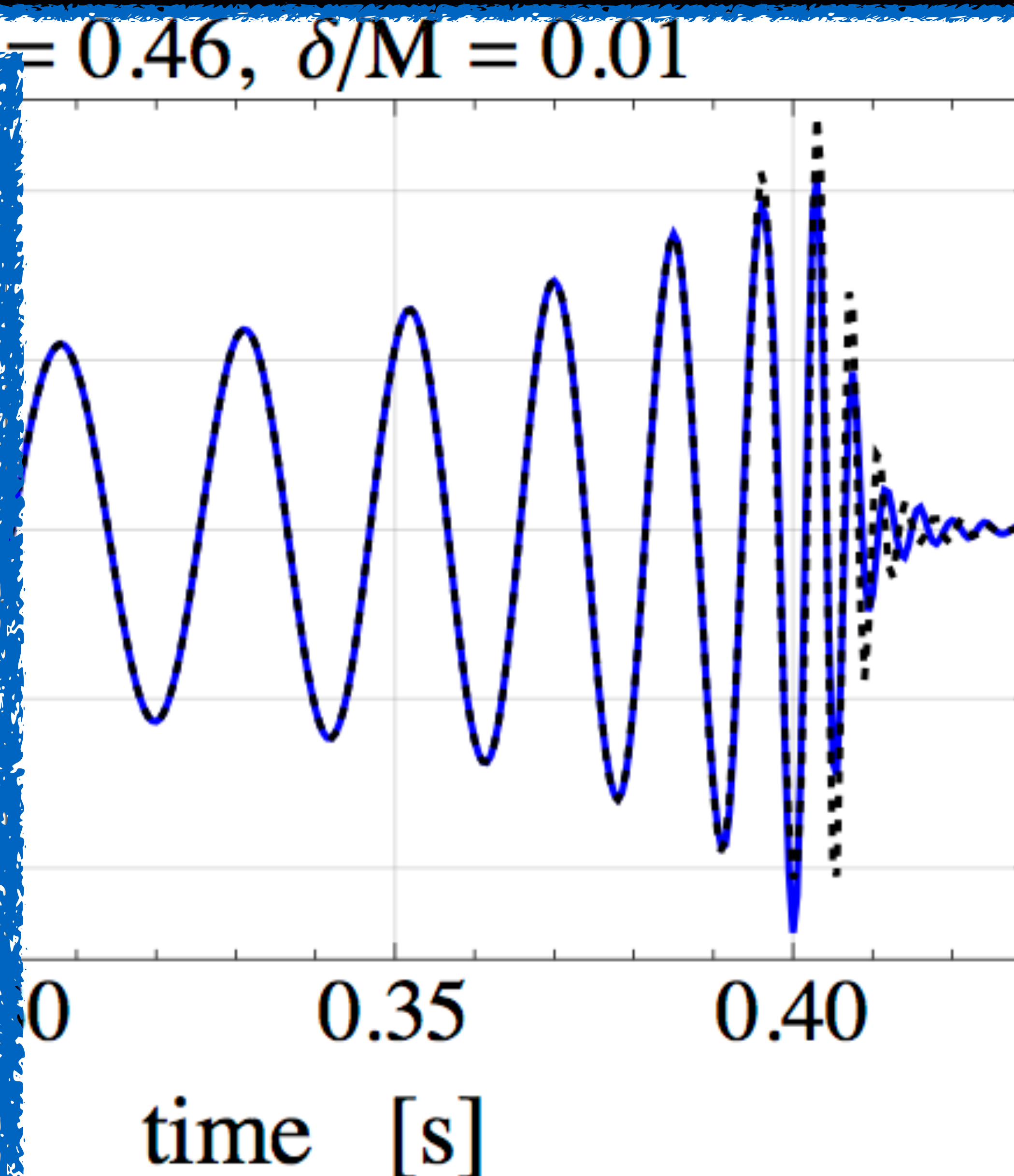

[arXiv:0706.1513]
[arXiv:1602.08759]
[arXiv:1602.07309]

PART IV

EXOTIC COMPACT OBJETCS

(background)

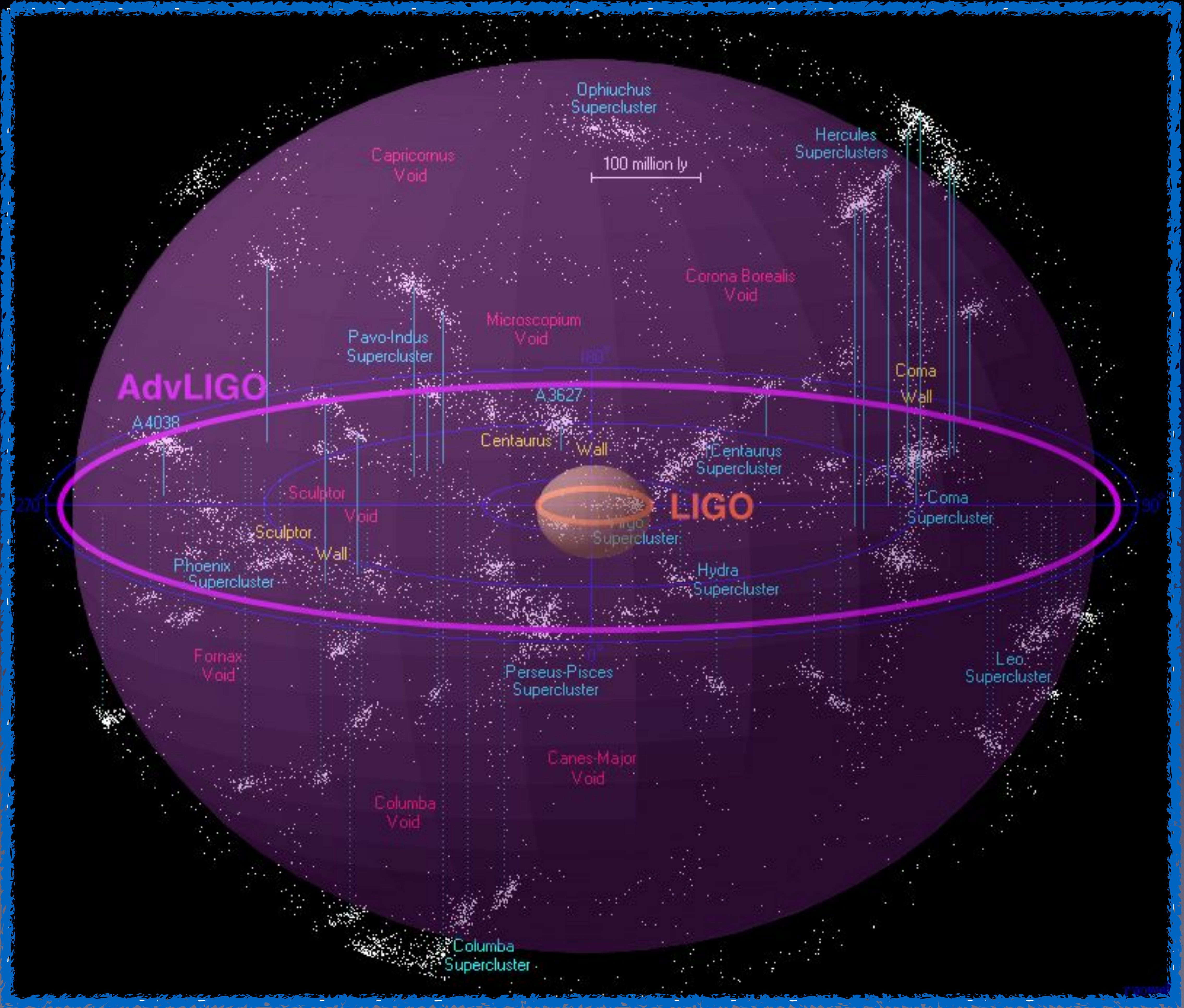

Ophiuchus Supercluster
Hercules Superclusters
Capricornus Void
100 million ly
Corona Borealis Void
Microscopium Void
Pavo-Indus Supercluster
AdvLIGO
A4038
A3627
Coma Wall
Centaurus
Wall
Centaurus Supercluster
Sculptor Void
Sculptor Wall
LIGO
Virgo Supercluster
Coma Supercluster
Phoenix Supercluster
Hydra Supercluster
270°
90°
Fornax Void
Perseus-Pisces Supercluster
Leo Supercluster
Canes Major Void
Columba Void
Columba Supercluster

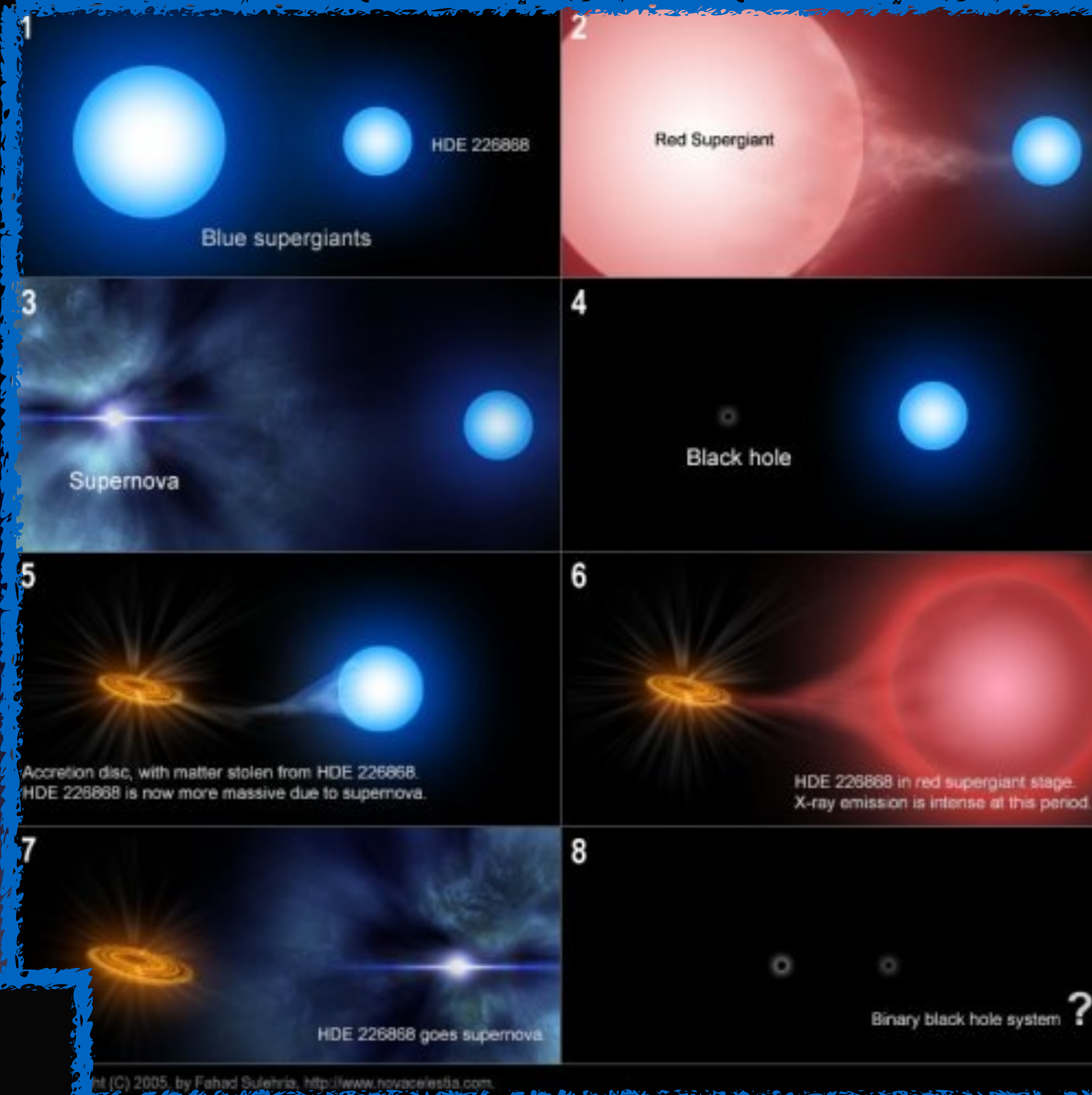
1
HDE 226868
Blue supergiants
2
Red Supergiant
3
Supernova
4
Black hole
5
Accretion disc, with matter stolen from HDE 226868.
HDE 226868 is now more massive due to supernova.
6
HDE 226868 in red supergiant stage.
X-ray emission is intense at this period.
7
HDE 226868 goes supernova
8
Binary black hole system ?
ht (C) 2005, by Fahad Sulehria, http://www.novacelestia.com.

www.eso.org

Model	Main physical properties and parameter variations
Standard	$M_{NS}^{max} = 2.5\ M_\odot$, *rapid* SN explosion, $\lambda =$ *Nanjing* [119], standard NS kick $\sigma = 265$ km s^{-1}, reduced BH natal kick, HG CE donor not allowed
Optimistic CE	HG CE donor allowed
Delayed SN	Delayed model for supernova explosions
High BH kicks	Full natal kick for BH

Further reading:
"Double compact objects I,II,III", Dominik et al.
[arXiv:1202.4901]
[arXiv:1308.1546]
[arXiv:1405.7016]

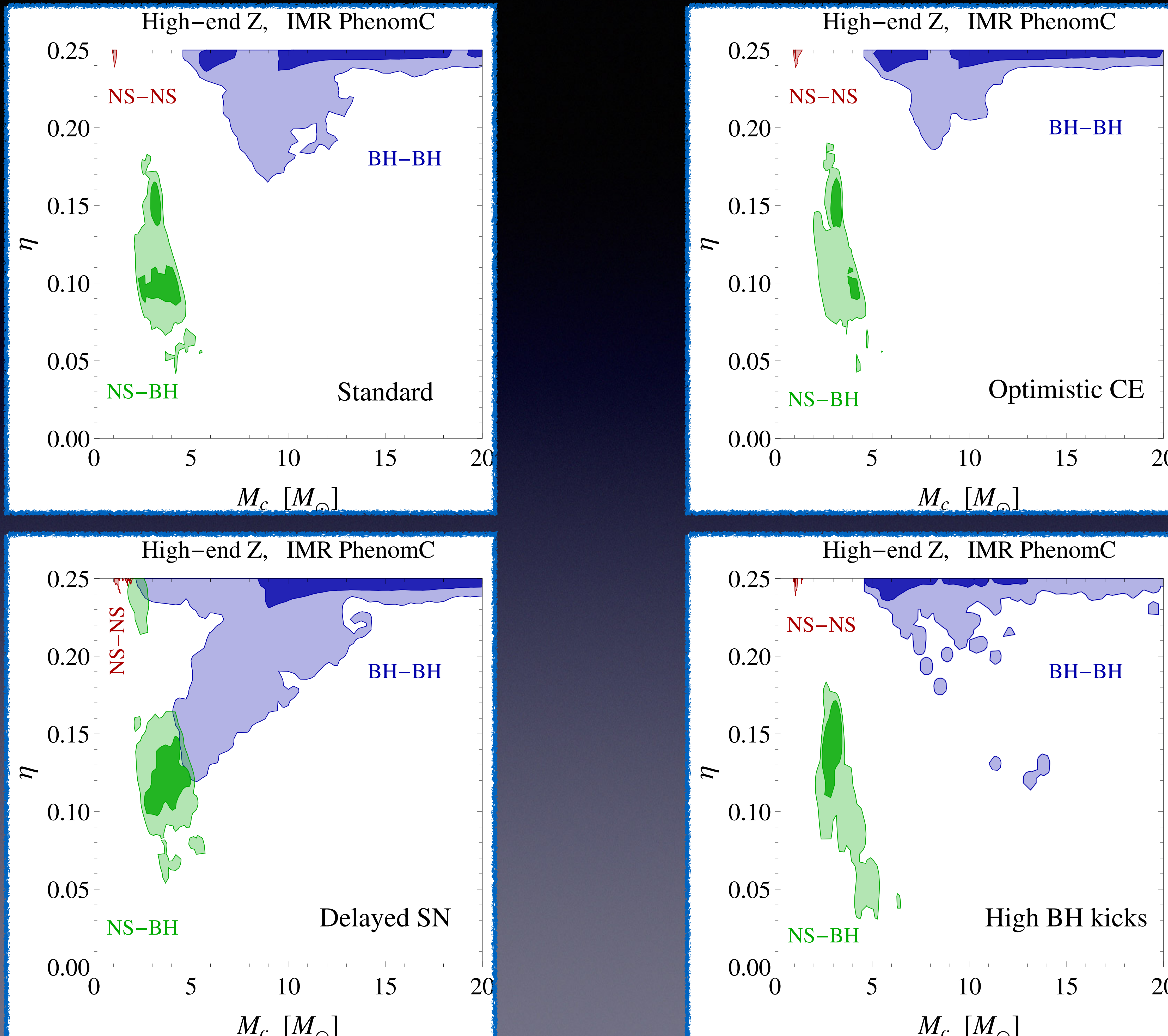
High−end Z, IMR PhenomC
NS−NS
BH−BH
NS−BH
Standard
η
M_c [$M_\odot$]
High−end Z, IMR PhenomC
NS−NS
BH−BH
NS−BH
Optimistic CE
η
M_c [$M_\odot$]
High−end Z, IMR PhenomC
NS−NS
BH−BH
NS−BH
Delayed SN
η
M_c [$M_\odot$]
High−end Z, IMR PhenomC
NS−NS
BH−BH
NS−BH
High BH kicks
η
M_c [$M_\odot$]

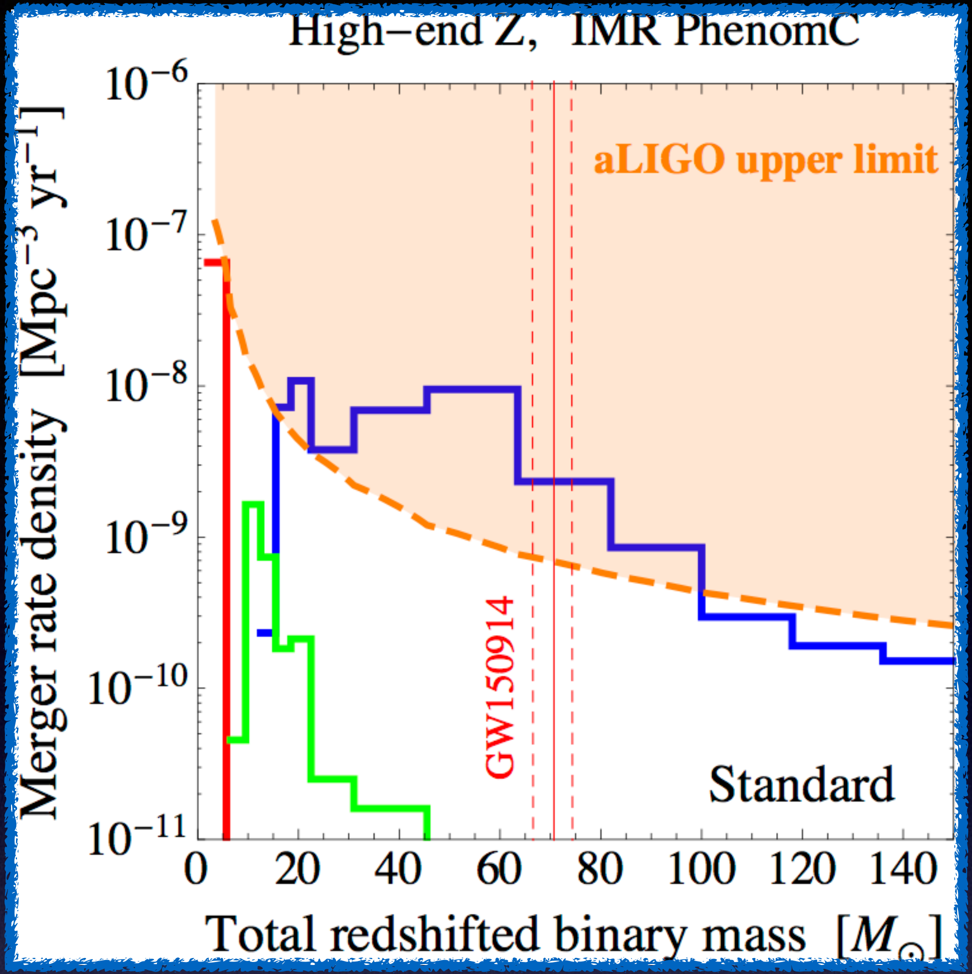
High−end Z, IMR PhenomC
aLIGO upper limit
GW150914
Standard
Merger rate density [Mpc^{-3} yr^{-1}]
10^{-6}
10^{-7}
10^{-8}
10^{-9}
10^{-10}
10^{-11}
0 20 40 60 80 100 120 140
Total redshifted binary mass [$M_\odot$]

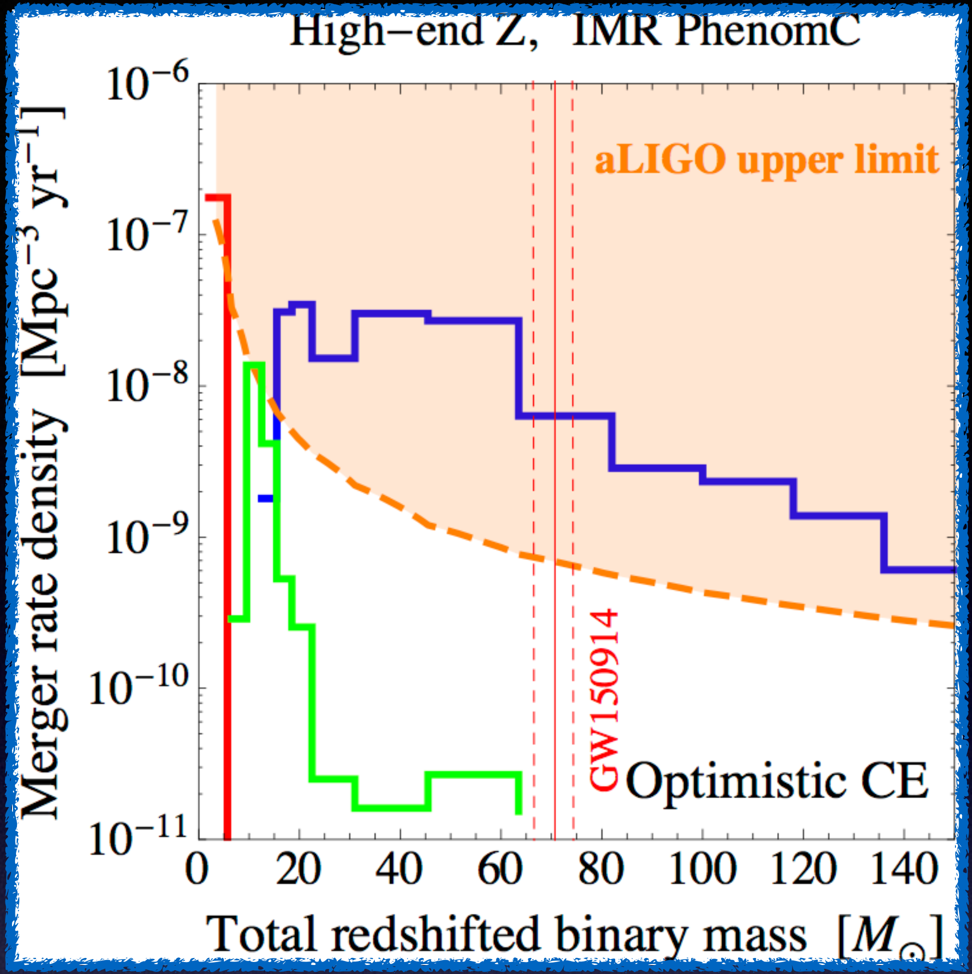
High−end Z, IMR PhenomC
aLIGO upper limit
GW150914
Optimistic CE
Merger rate density [Mpc^{-3} yr^{-1}]
10^{-6}
10^{-7}
10^{-8}
10^{-9}
10^{-10}
10^{-11}
0 20 40 60 80 100 120 140
Total redshifted binary mass [$M_\odot$]

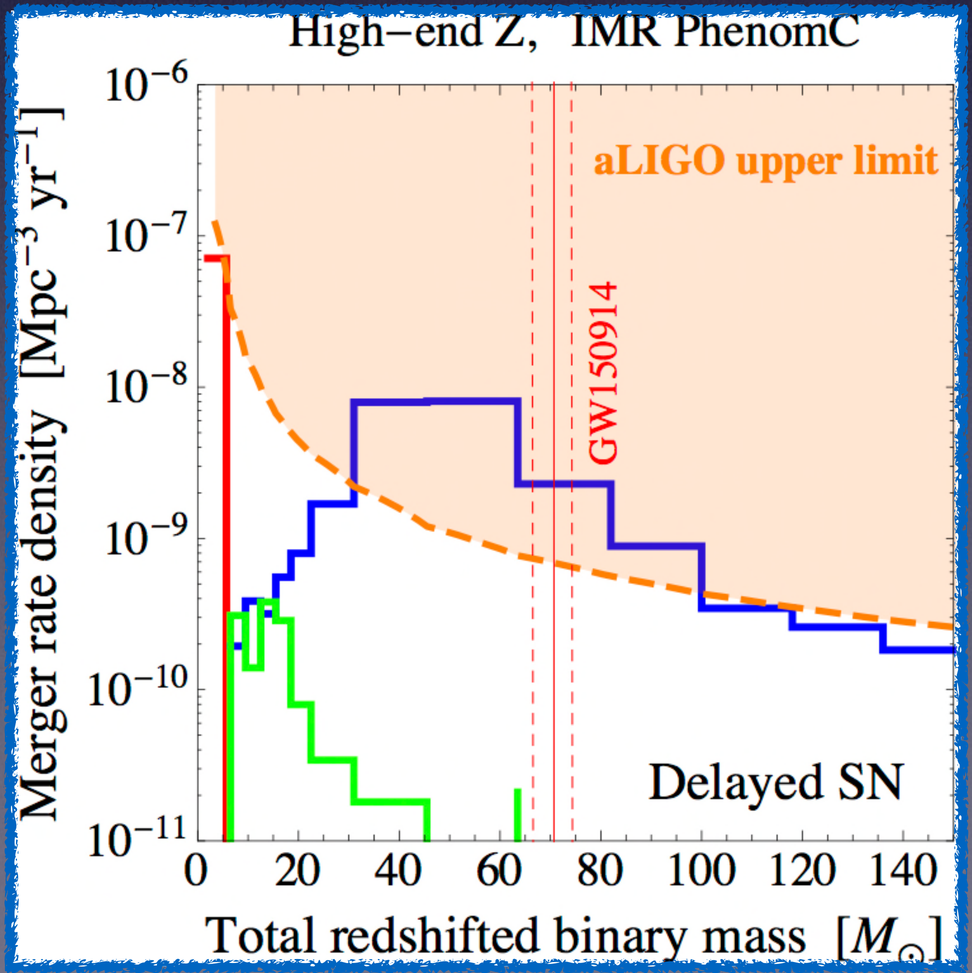
High−end Z, IMR PhenomC
aLIGO upper limit
GW150914
Delayed SN
Merger rate density [Mpc^{-3} yr^{-1}]
10^{-6}
10^{-7}
10^{-8}
10^{-9}
10^{-10}
10^{-11}
0 20 40 60 80 100 120 140
Total redshifted binary mass [$M_\odot$]

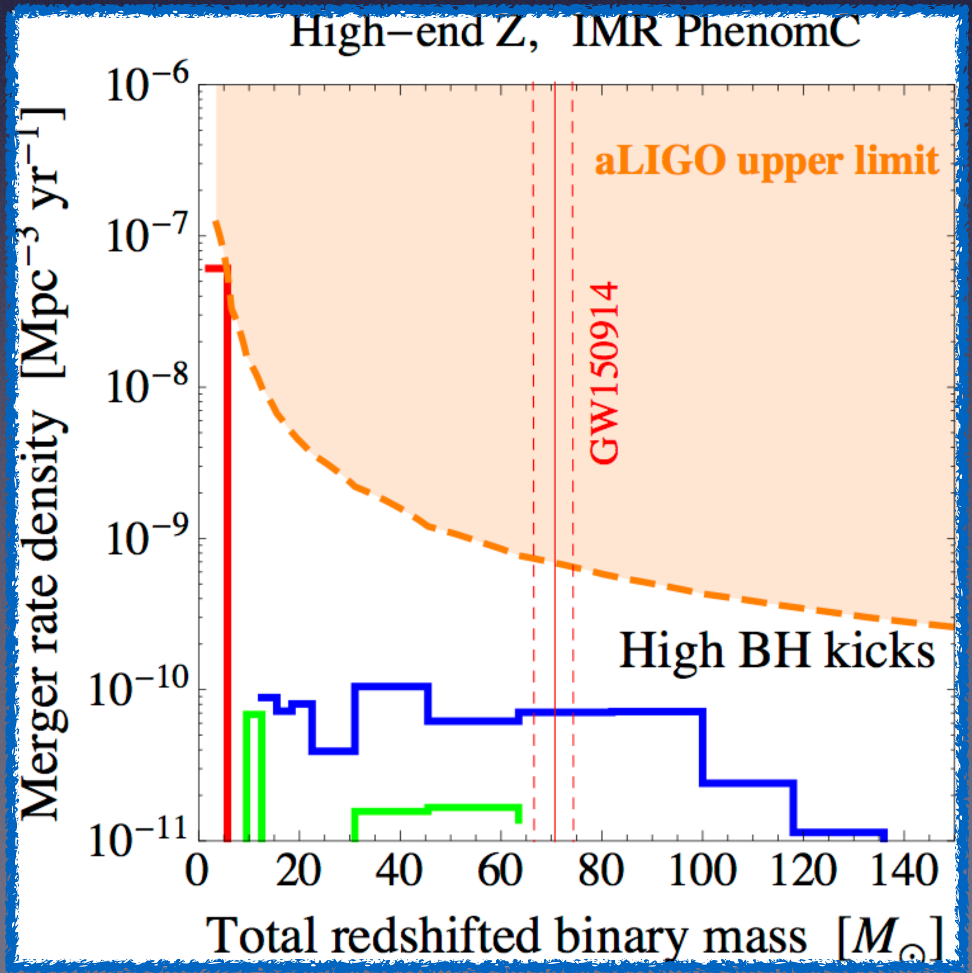
High−end Z, IMR PhenomC
aLIGO upper limit
GW150914
High BH kicks
Merger rate density [Mpc^{-3} yr^{-1}]
10^{-6}
10^{-7}
10^{-8}
10^{-9}
10^{-10}
10^{-11}
0 20 40 60 80 100 120 140
Total redshifted binary mass [$M_\odot$]

PART V

CONCLUSIONS

- See more at: http://www.ligo.org/science.php

Humans have mainly relied on different forms of light to observe the Universe. Today, we are on the edge of a new frontier in astronomy: GW astronomy.

Gravitational waves carry information on the motions of objects in the Universe. Since the Universe was transparent to gravity moments after the Big Bang and long before light, GWs will allow us to observe further back into the history of the Universe than ever before.

Most importantly, GWs hold the potential of the unknown. Every time humans have opened new "eyes" on the Universe, we have discovered something unexpected that revolutionized how we saw the universe and our place within it.